Dynamic behavior of pile-supported structure on a liquefiable slope

Nghiem Xuan Tran[1], B.-S. Yoo[1], S.-R. Kim[1*], and W.-J. Park[2]

[1] Department of Civil and Environmental Engineering, Seoul National University, 1 Gwanak-ro, Gwanak-gu, Seoul 08826, South Korea.
[2] Nambu Regional Construction Headquarters, Korea Electric Power Corporation, 21, Bosoodae-Ro, Seo-Gu, Busan 49247, South Korea.

ABSTRACT

Evaluating lateral-spreading force that acts on piles is an interesting topic in the design of pile foundations on a liquefiable sloping ground. In this study, the effects of initial and kinematic forces on pile responses were examined through centrifuge model test. A single pile and a 2×2 pile group were installed into saturated sandy ground. The liquefiable sloping ground with an inclination angle of 27° was prepared to simulate the triggering of the lateral spreading. The model was excited at the container base using a ramped sinusoidal wave of 1.5 Hz frequency. The initial force induced the largest transient lateral displacement of decks and bending moment exerted on piles within the first few cycles. Significant development of lateral spreading force associated with the decrease in transient amplitude resulted in considerable monotonic deck displacement and bending moment. Thus, the interaction between initial and kinematic forces can be decomposed in the preliminary design.

Keywords: single pile; group pile; sloping ground; saturated sand; kinematic loading

1 INTRODUCTION

Pile foundations are widely used to support large structures located on weak strata. Pile-supported wharf, which is composed of a deck and supporting piles, is an important type of pile foundation used for offshore structures. The wharf is usually founded on a sloping and young deposit that is susceptible to liquefaction. Medium and strong earthquakes have frequently occurred over the past decades, damaging numerous wharves extensively (PIANC 2001).

The two loading conditions for pile foundation on a liquefiable slope are inertial loading, which is induced by structural masses; and kinematic loading, which is induced by lateral ground deformation. The interaction between these two loadings remains an interesting issue. For example, according to Caltrans (2012) and AASHTO (2014), inertial and kinematic effects should be simultaneously considered. Other design codes, such as ASCE CORPI 61-14 (2014) and POLB (2015), recommend that these effects be evaluated on a project-specific basis. Considering results obtained from simplified analysis, Souri et al. (2018) suggested that full interaction between kinematic and inertial demands could be considered within shallow depth (less than 10 diameters below the ground surface).

The experimental approach has been employed to explore the seismic behavior of pile-supported wharves. McCullough et al. (2003) and McCullough et al. (2007) performed five pile-supported wharf models representing the common wharf configuration using the centrifuge technique. Pile foundation performed poorly due to the presence of weak soils and large bending moments at the interface between soft and stiff soil layers. A centrifuge test program at a centrifugal acceleration of 50 g was conducted by Takahashi and Takemura (2005) to simulate the observed damage of Takahama wharf in Kobe Port, Japan. The authors argue that the large bending moments on piles were due to large horizontal movement of liquefiable soils as a result of liquefaction. Attempting to simulate those case histories proves that centrifuge modeling can capture the actual seismic response of pile-supported wharves.

The current study aims to improve the understanding of the complicated dynamic interaction among soils, piles, and structures by performing a centrifuge model test. The centrifuge test was conducted on the single pile and pile group installed in a liquefiable sandy slope. The seismic behavior of the testing model was analyzed in terms of ground response, deck displacement, and bending moment distributed along the pile length. The combination of inertial and kinematic forces acting on piles is discussed in this paper to provide practical design recommendations.

2 CENTRIFUGE MODELING

2.1 Centrifuge modeling

A centrifuge machine with approximately 5 m of arm length was employed for the centrifuge test at the Korea Advanced Institute of Science and Technology. The testing model was built in an equivalent shear beam (ESB) container, which can minimize the reflection effect of the container wall. The ESB

container was 65 cm wide, 65 cm long, and 65 cm high. The capability and applicability of the centrifuge machine and ESB container in simulating seismic response were reported by Lee et al. (2012).

A length scaling factor of 34 was applied in this study. Other scaling factors were derived following suggestions by Wood (2004) and Madabhushi (2014). Pure water was used as pore fluid. All data are presented in prototype scale unless stated otherwise.

A 2×2 pile group was designed to simulate a wharf prototype segment, as shown in Fig. 1. In addition, a single pile was constructed in the same soil box to compare with the dynamic behavior of the group pile. Aluminum alloys were used to create model decks and piles. The model pile was 0.85 m in diameter (*D*), 0.068 m in thickness, and 18 m in length. Deck 1 (mounted pile group) was 7.14 m long, 7.14 m wide, and 0.99 m thick. Deck 2 (mounted on the single pile) was designed to support one-fourth of the mass of the pile group. All structures were installed in saturated loose silica sand with an inclination of 27° (Fig. 1).

Single pile and two piles of the group (SP, GP1, and GP2 in Fig. 1) were instrumented with strain gauges to obtain the bending moment response during testing. Calibration tests were conducted to determine the flexural stiffness (*EI*) of these model piles.

2.2 Model preparation

The loose liquefiable ground was prepared via water sedimentation method. Prior to making ground, accelerometers and pore pressure transducers were mounted using several strings and flexible steel bars. First, these steel bars and model piles were fixed to a plate, which was then fixed onto the bottom of the container. Second, the saturated silica sand, which was submerged for more than 24 h, was poured to the ESB container through a No. 10 sieve. The water level was then lowered to make the slope surface. Finally, the water level was raised to the design height, and all decks were rigidly connected to the pile heads.

A total of four linear variable differential transformers (LVDTs) were used to measure the lateral displacement of structures and the settlement of the ground surface. A sinusoidal wave with ramped amplitude and a frequency of 1.5 Hz was applied at the base of the ESB container to examine the dynamic behaviors of both structures, as shown in Fig. 2. The maximum amplitude of the applied motion was approximately 0.2 g. The configuration of the model before and after testing was also measured to analyze the permanent ground deformation.

3 TEST RESULTS AND ANALYSES

3.1 Ground response

The time histories of EPWP had insignificant fluctuation, which indicated that dilation phenomenon might not occur in the experiment. The time histories of ground acceleration and excess pore water pressure (EPWP) responses are shown in Figs. 3 and 4, respectively. The ground response can be divided into two stages: Stage 1 (0 to 12 s) prior to maximum EPWP and Stage 2 (12 s to end of shaking).

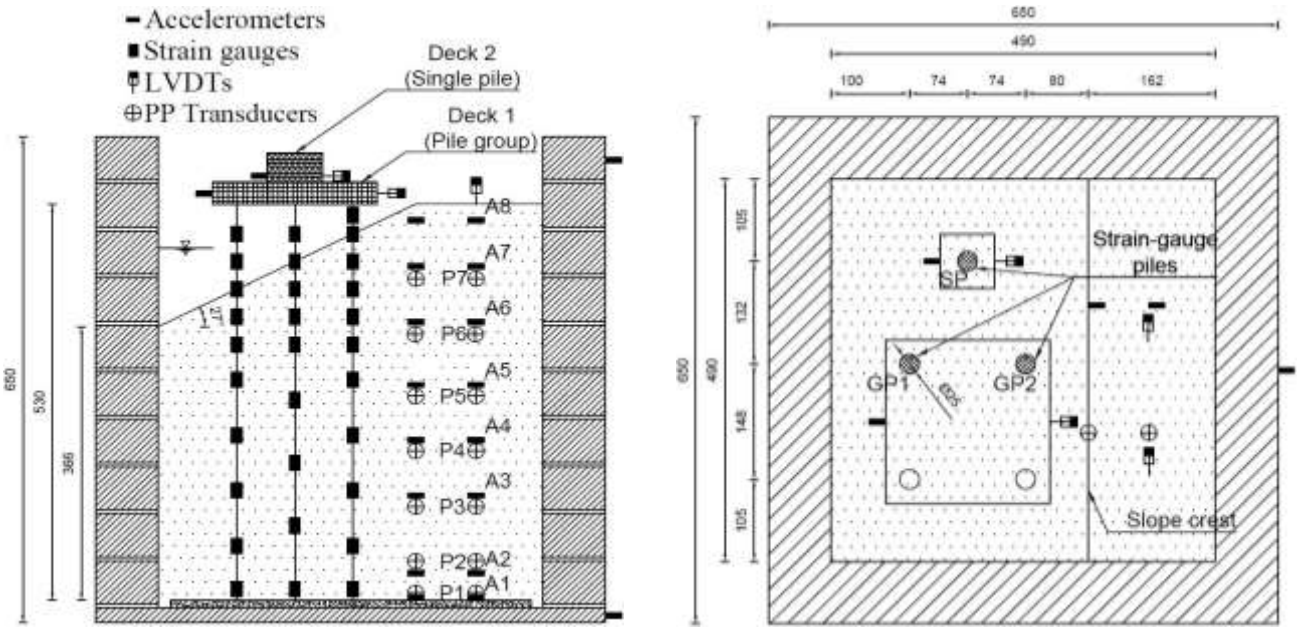

a) Side view

b) Top view

Fig. 1. Layout of the model test.

In Stage 1, the input acceleration was amplified when propagating from the container base to the ground surface in association with the rapid development of EPWP. The top two acceleration time histories (A8 and

A7) behaved differently because the corresponding accelerometers were located in the unsaturated region. When the EPWP reached the maximum value, the response accelerations started attenuating slightly (Stage 2) due to the loss of soil stiffness. The time histories of EPWP had insignificant fluctuation. Thus, dilation phenomenon might not occur in the experiment.

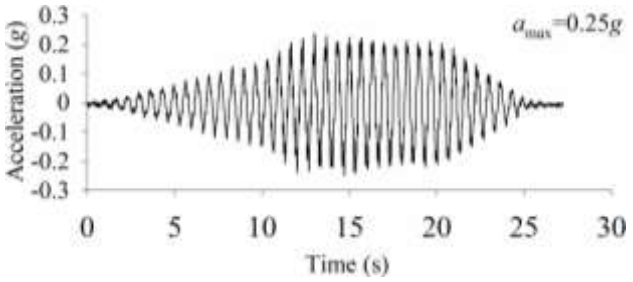

Fig. 2. Raw time history of input acceleration.

3.2 Deck response

The behavior of deck displacements was described in two forms, as shown in Fig. 5: (1) transient component only obtained through double integration of deck accelerations, and (2) a combination of transient and monotonic components obtained from LVDT measurements. The transient displacements of Decks 1 and 2 reached maximum values after 8 and 7 cycles, respectively, as shown in Fig 5(a). The maximum transient displacement of Deck 2 was approximately 1.8 times larger than that of Deck 1. Thereafter, the transient of both decks started decreasing to approximately 10 s close to the time of the maximum EPWP. This behavior was consistent with the rapid development of pore water pressure, which caused a considerable reduction in soil stiffness.

After 10 s, the transient displacement of Deck 2 increased slightly within 5 cycles and then continued decreasing its amplitude until the end of shaking. By contrast, after attaining minimum value, the transient displacement of Deck 1 started increasing continuously following the pattern of input motion. The distinct behavior of transient displacement between two decks might be attributed to the difference in the foundation stiffness. The pile group with much larger foundation stiffness could vibrate in accordance with the predominant input motion, even though the soil began to flow around the piles.

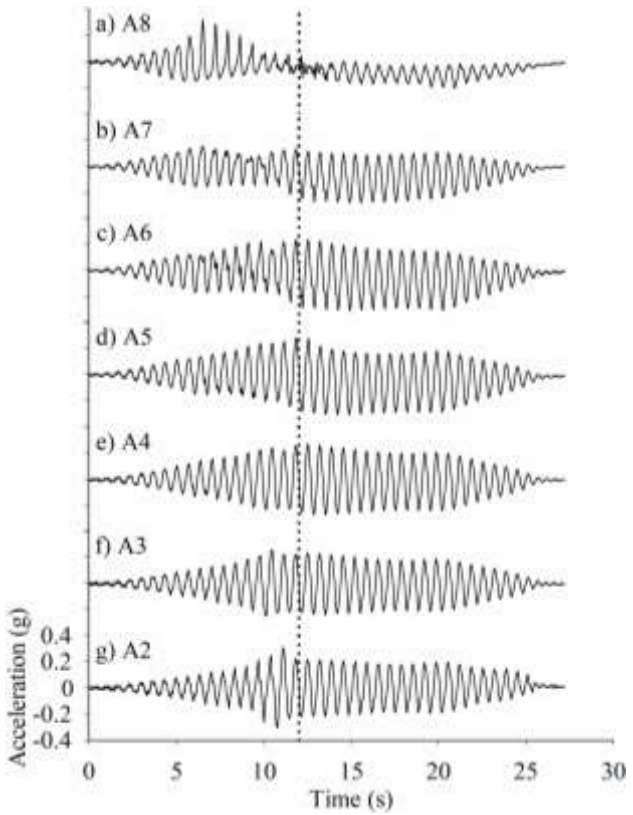

Fig. 3. Time histories of ground acceleration responses.

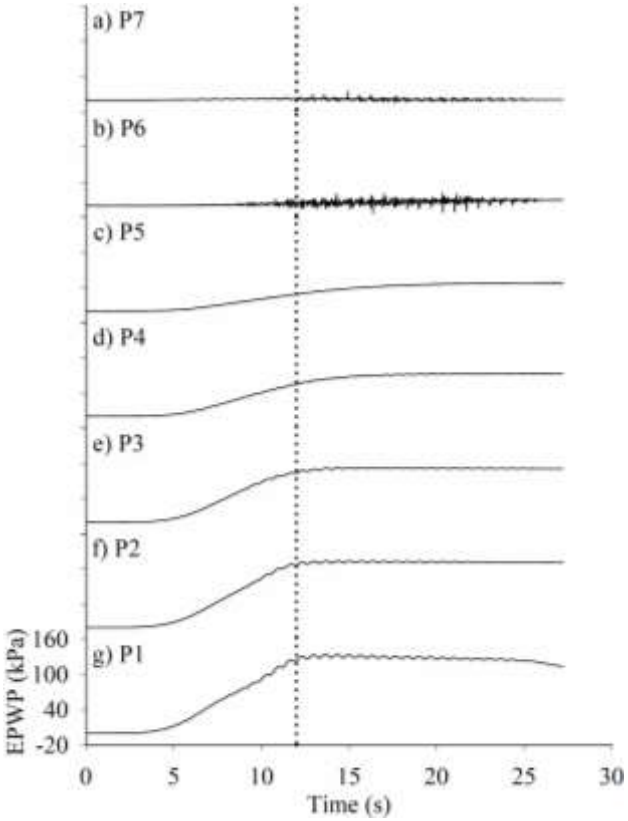

Fig. 4. Time histories of excess pore pressure responses.

The effect of slope failure on the deck displacements is presented in Fig. 5(b). Decks 1 and 2 reached the maximum values at or close to the time of maximum excess pore pressure. The maximum

displacement of Deck 2 (approximately 35.2 cm) was 3.2 times larger than that of Deck 1 (approximately 11.1 cm). The single pile with smaller foundation stiffness suffered a large displacement in the downslope direction because of the significant development of kinematic loading. Both decks eventually bounced back to the original configuration according to the disappearance of kinematic loading.

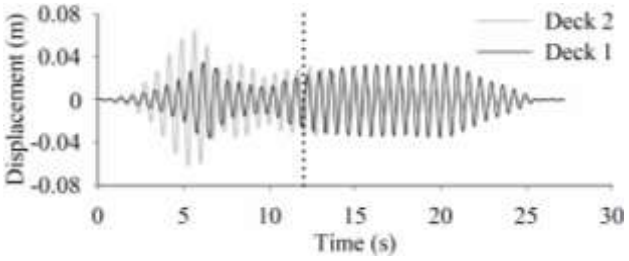

a) Transient component

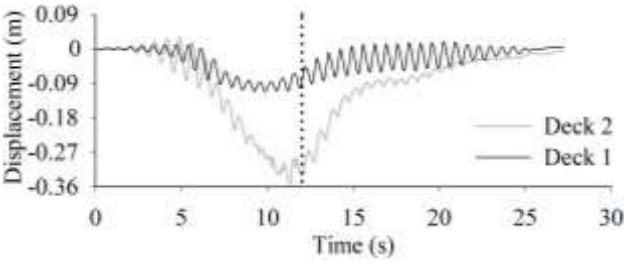

b) Transient and monotonic components

Fig. 5. Time histories of deck displacements.

3.3 Pile response

Bending moment variation was derived from strain recordings based on pile curvature. The time histories of bending moment variation near the pile toe and head of all instrumented piles are illustrated in Fig. 6. Close to the time of the maximum EPWP, the bending moment of group piles attained the maximum values at both ends according to the fixed conditions, whereas only the bending moment of the single pile at the toe reached the maximum value. The maximum bending moment of GP1 was approximately 1.1 times larger than that of GP2 because GP1 had a long unsupported length. The maximum bending moment of SP at the toe (around 2500 kN·m) was about 2 times larger than that of GP1 and GP2 (about 1300 kN·m).

The bending moment near the pile head was dominant with the transient and monotonic components. For group piles, the amplitude of the bending moment near the pile head reached a maximum value at few cycles and slightly decreased to 12 s. Then, the amplitude increased again according to the loss of soil stiffness. By contrast, the amplitude of the bending moment near the pile head of the single pile continued decreasing after attaining the maximum value. However, the bending moment near the pile toe was dominant by monotonic component, which was induced by lateral spreading. The transient component of the bending near the pile toe behaved in the same manner as that near the pile head. In conclusion, the behavior of moment was consistent with the deck responses, which were governed by the initial force of deck masses and kinematic loading of lateral spreading.

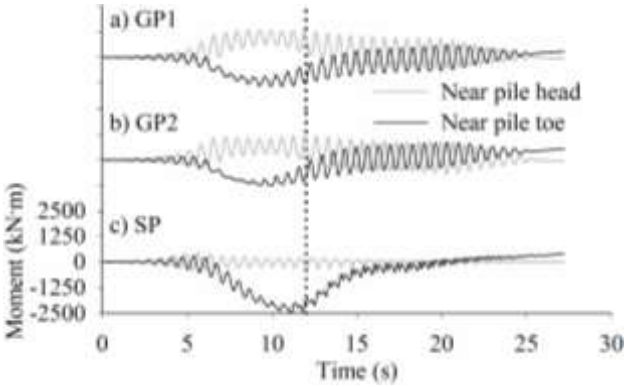

Fig. 6. Time histories of bending moment responses.

3.4 Effect of lateral spreading on pile response

The time history of deck displacement could be divided into two components, namely, monotonic and transient, as shown in Fig. 7. In this study, the monotonic component was computed by applying fast Fourier transform smoothing with a cutoff frequency of approximately 0.89 Hz. Then, the transient component was calculated by subtracting the monotonic component from the recorded lateral displacement.

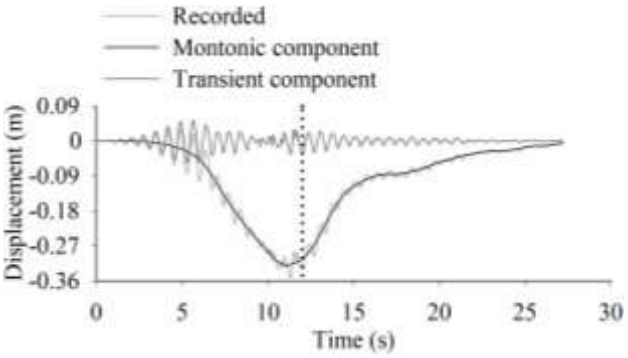

Fig. 7. Decomposition of lateral displacement of Deck 2.

The correlation between the ground surface settlement and monotonic lateral displacement of Deck 2 is shown in Fig. 8. The settlement continued to increase after the end of shaking due to the dissipation of EPWP. The final settlement was manually measured at about from 2.45 m to 2.65 m. The ground surface settlement is related to the development of lateral spreading force imposed on piles. The effect of lateral spreading force on piles is represented by the monotonic component of lateral displacement of decks.

As EPWP rapidly developed until 12 s (Fig. 4), the settlement increased almost linearly with time. Thus, the lateral spreading force acting on piles might

increase in a similar manner, i.e., the monotonic lateral displacement increased proportionally in the downslope direction (Fig. 8). By contrast, when the EPWP reached the maximum value, the sandy ground became partially softened. The contact between the soil and pile was weakened, which led to the reduction of lateral spreading force exerted on piles. Therefore, after reaching the maximum value at 12 s, the monotonic lateral displacement of decks bounced back to the original position.

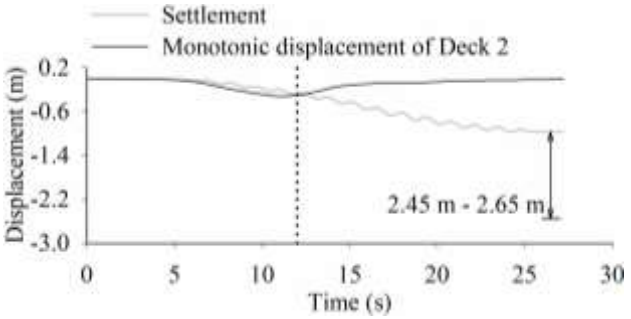

Fig. 8. Correlation between ground surface settlement and monotonic of ground displacement of Deck 2.

4 CONCLUSION

Seismic response of the single pile and pile group on liquefiable sloping ground was assessed via centrifuge modeling. The centrifuge model was excited at the base with a ramped sinusoidal wave of 1.5 Hz frequency. By decomposing the time history of structural responses into monotonic and transient components, the inertial force induced the largest transient lateral displacement of decks and bending moment exerted on piles within the first few cycles. Very large monotonic deck displacement and bending moment then became almost consistent with the time instant of the maximum EPWP, i.e., significant development of lateral spreading force imposed on piles in the downslope direction. The deck lateral displacement and bending moment eventually bounced back to the original configuration after reaching the maximum value as the soil partially softened in association with the maximum EPWP. Therefore, the interaction between initial and lateral spreading forces can be decomposed in the preliminary design.

ACKNOWLEDGEMENTS

This research was supported by the project entitled “Development of performance-based seismic design technologies for advancement in design codes for port structures,” funded by the Ministry of Oceans and Fisheries of Korea.

REFERENCES

American Association of State Highway and Transportation Officials (AASHTO) (2014). Guide Specifications for LRFD Seismic Bridge Design, Second Edition with 2014 Interim, AASHTO, Washington, D.C.

American Society of Civil Engineers/Coasts, Oceans, Ports, and Rivers Institute (ASCE/COPRI) 61-14 (2014). Seismic Design of Piers and Wharves, prepared by the ASCE Standards Comm. on Seismic Design of Piers and Wharves, ASCE, Reston, VA.

California Department of Transportation (Caltrans) (2012). Guidelines for Foundation Loading and Deformation Due to Liquefaction Induced Lateral Spreading, Sacramento, CA.

Lee, S.H., Choo, Y.W., and Kim, D.S. (2013). Performance of an equivalent shear beam (ESB) model container for dynamic geotechnical centrifuge tests. Soil Dynamics and Earthquake Engineering, 44:102-114.

Madabhushi, G. (2014). Centrifuge Modelling for Civil Engineering, CRC Press.

McCullough, N.J. (2003). The Seismic Geotechnical Modeling, Performance, and Analysis of Pile-Supported Wharves, PhD Dissertation, Oregon State University, Corvallis.

McCullough, N.J., Dickenson, S.E., Schlechter, S.M., and Boland, J.C. (2007). Centrifuge Seismic Modeling of Pile-Supported Wharves. Geotechnical Testing Journal, 30(5): 349–359.

Permanent International Association of Navigation Congresses (PIANC) (2001). Seismic Design Guidelines for Port Structures, Permanent International Navigation Association, A.A. Balkema Publishers, Rotterdam, Netherlands.

Port of Long Beach (POLB) (2015). Port of Long Beach Wharf Design Criteria, POLB WDC Version 4, May 2015.

Souri, M., Khosravifar, A., Dickenson, S.E., Schlechter, S., and McCullough, N. (2018). Inertial and Liquefaction-Induced Kinematic Demands on a Pile-Supported Wharf: Physical Modeling. Geotechnical Earthquake Engineering and Soil Dynamics V GSP 292, Volume 3: Numerical Modeling and Soil Structure Interaction, ASCE, New York, 388–397.

Takahashi, A. and Takemura, J. (2005). Liquefaction-induced Large Displacement of Pile-Supported Wharf. Soil Dynamics and Earthquake Engineering, 25(11): 811–825.

Wood, D.M. (2004). Geotechnical modeling, CRC Press.